

Formation and Evolution of Young Massive Clusters

Bruce G. Elmegreen

IBM Research Division, T.J. Watson Research Center, 1101 Kitchawan Road, Yorktown Hts., NY 10598, USA, bge@watson.ibm.com

Abstract. Clusters are the dense inner regions of a wide-spread hierarchy of young stellar structures. They often reveal a continuation of this hierarchy inside of them, to smaller scales, when they are young, but orbital mixing eventually erases these subparts and a only smooth cluster or smooth unbound group remains. The stellar hierarchy follows a similar structure in the interstellar gas, which is presumably scale-free because of supersonic motions in the presence of turbulence and self-gravity. The efficiency of star formation increases automatically with density in a hierarchical ISM, causing most dense stellar groups to be initially bound for local conditions. In lower pressure environments, the infant mortality rates should be higher. Also following from hierarchical structure is the cluster mass distribution function and perhaps also the cluster size distribution function, although the predicted mass-size relation is not observed. Cluster destruction is from a variety of causes. The destruction time should depend on cluster mass, but the various groups who have studied this dependence have gotten significantly different results so far.

1. Introduction: Cluster Basics

1.1. Hierarchical structure in young star fields

We know what a cluster is when we see one, but there is a lot more to clustering than meets the eye. Embedded clusters often contain sub-clusters, for example, and clusters generally cluster together themselves into double clusters or star complexes. Taken together, there is a hierarchy of young stellar structures, with the objects commonly called clusters representing only the inner and denser parts of the hierarchy. Presumably the main difference between the clusters and the rest of the hierarchy is that the clusters have had sufficient time and gravitational self-attraction to get mixed by stellar orbital motions. The rest of the hierarchy could partially mix later, by cluster coalescence, for example, or it could disburse through tidal forces.

The subclustering of clusters is evident when the clusters are still young in terms of their dynamical time. Examples are NGC 2264, which has four subclusters with slightly different ages (± 1 My; Dahm & Simon 2005), rho Oph (Smith et al. 2005), and Serpens (Testi et al. 2000). Not all clusters will be born with clear sub-clustering. If a cloud core has a strong radial density gradient, then primordial gas subclustering can be erased or mixed by tidal forces (for the same reason that clouds with strong density gradients will not fragment much during free fall collapse). However, cloud cores with strong density gradients are already fairly old when measured in gas dynamical times; i.e., they have had

at least a crossing time to respond to self-gravitational forces. In these cases, the hierarchy of the gas is smoothed over somewhat by dynamical motions even before star formation begins. Nevertheless, the cluster that results is the mixed inner region of the hierarchy, with the mixing occurring mostly in the gas phase rather than the stellar phase in this case with a strong gradient.

On larger scales, young stars cluster together in unbound structures, like OB associations. Efremov (1995) has studied such large scale clustering for 30 years. Most recently, Ivanov (2005) mapped the star complexes in M33 and Bastian et al. (2005) studied cluster complexes in M51. There is no characteristic length or mass scale for these larger structures; the distribution functions for their luminosity and size are power laws (Elmegreen et al. 2006, and references therein). An OB association has a characteristic size of about 80 pc (Efremov 1995), but this is only because of a selection effect: There is a general correlation between the duration of star formation and the size of the region, and OB associations are selected as concentrations of OB stars. This limits their age to ~ 10 My and thereby limits their size to the observed 80 pc (Efremov & Elmegreen 1998). Collections of older stars, such as red supergiants or Cepheid variables, are larger, 650 pc according to Efremov (1995). Collections of younger stars, such as pre-main sequence stars, are smaller (in embedded clusters). The origin of the correlation is probably turbulence, because the ratio of the size to the age, which is a velocity, correlates with the size like the linewidth-size relation for molecular clouds, having about the same slope and intercept (Elmegreen 2000).

Clusters have been defined *historically* as small, gravitationally bound, isolated collections of stars; their density exceeds the local tidal density. By the time the objects appear as “clusters,” the stars in them are mixed along with most previous subclusterings, and the peripheral stars are dispersed. Thus they tend to look isolated and unique. In fact they are not born that way, they are born as part of a hierarchy of young stellar structures without much distinction other than their location in the high density parts.

Simulations of collapsing clouds by Bonnell, Bate & Vine (2003) show hierarchical star formation with clusters in several dense cores. These clusters mix together over time making larger clusters. The observations do not yet clearly distinguish between clouds like these that are collapsing freely and clouds that have some level of radial stability resulting from magnetic forces or isotropic turbulent motions. Quasi-stability seems favored by observations of cloud core self-absorption where the absorption line redshift is only $\sim 20\%$ of the linewidth (Myers et al. 2000). Such small redshifts suggest that cloud cores are contracting relatively slowly, on a time scale of several radial-crossing times. However, recent observations of global infall in NGC 1333 (Walsh, Bourke, & Myers 2006) suggest dynamical processes on shorter times, similar to those envisioned by Bonnell, Bate & Vine (2003). In either case, the stars should form in a hierarchical way (Sect. 1.6.).

1.2. Hierarchical structure in the gas

Interstellar gas has a similar hierarchy of structures. Power spectra of gas emission show power laws, indicating no characteristic scale (Dickey et al. 2001). The power spectra of optical light in a galaxy is about the same as the power

spectrum of interstellar gas (Elmegreen et al. 2003). These results suggest that the stars follow the gas when they form, although extinction may contribute to the optical power spectrum too. In terms of cloud-like objects, the highest level in the hierarchy, on the largest scale, consists of giant atomic clouds that contain $\sim 10^7 M_{\odot}$ of gas. These are evident in the Milky Way (McGee & Milton 1964; Elmegreen & Elmegreen 1987) and in local galaxies where HI maps have the resolution needed to see them (e.g., Boulanger & Viallefond 1992). Molecular clouds are the next denser level in the hierarchy of structures, and they often collect together inside the atomic clouds if the ambient pressure is large enough to allow molecules to form (Elmegreen 1993; Blitz & Rosolowsky 2006). Maps in Grabelski et al. (1987) show this GMC collection clearly for the Milky Way. Inside giant molecular clouds are cloud cores, and so on down to the smallest scales that can be observed.

It is worth making the cautionary note that this hierarchical structure for both gas and stars does not mean every small object is inside a larger one. Small objects can be to the side of large objects, with no obvious larger scale structures around them. Most objects do contain substructures, however, down to or below the scale where thermal motions dominate (or random stellar motions dominate in the case of stellar clustering). An example of this type of structure is illustrated in Figure 1, below.

1.3. Star Formation Efficiency

Individual stars form at the bottom of the hierarchy, where the gas is in the form of dense clumps. As we consider lower and lower levels in the hierarchy, i.e., as the average gas density gets higher, the mass fraction in the form of the dense star-forming clumps goes up. On the scale of the clumps themselves, the mass fraction is unity. On the scale of the GMC, the mass fraction is small because there is a large volume of low-density gas between the cores and even more between the clumps. This is the nature of the hierarchy, which is fractal. Stars form inside each clump at some average efficiency, which may be about constant, perhaps one-third or one-half (e.g., Matzner & McKee 2000). Thus the overall efficiency of star formation, which is the mass fraction of a cloud that turns into stars, increases towards higher gas density inside the cloud. This is why the efficiency in a cloud core may be 20% or 30%, but the efficiency for a whole OB association is only 5%. The OB association is the result of star formation inside the densest clumps of a GMC, but there is a lot of low-density intercore and interclump gas in a GMC that does not form stars.

We see now another aspect of cluster formation: in the dense regions of the hierarchy where clusters form (GMC cores), the mass fraction in the form of individual star-forming clumps is automatically high, so the efficiency of star formation is automatically high. This means that the stars have a high probability of ending up gravitationally bound together. High average density and boundedness go together; one follows from the other in a hierarchical interstellar medium. The high efficiency needed for bound cluster formation is not the result of special circumstances related to the stars themselves, such as feedback processes, but only the result of hierarchical gas structure. At the density that is high enough to form a compact region of stars, one that stands out to the eye as a star cluster, the efficiency of star formation is automatically high.

1.4. Theory of Cluster Formation

Putting these concepts together, we can get most of the way toward explaining the origin of star clusters: they are the inner mixed regions of the young-star hierarchy, where the dynamical time is short and the age is comparable to or longer than this dynamical time (to ensure mixing). Because most star formation occurs in only a few dynamical times, a high fraction of the clumps will have formed stars by the time mixing has occurred, and because the clumps represent a high fraction of the local gas mass in a cloud core, the efficiency of star formation is generally high there. Then the mixed stellar regions remain gravitationally bound after the gas leaves. Thus bound clusters are an inevitable result of star formation in hierarchically structured gas for ISM properties like those in the Solar neighborhood.

1.5. Bound versus unbound clusters

This initial binding does not mean that young clusters stay bound for long. Ninety percent lose a high fraction of their stars within the first 10 My (Lada & Lada 2003; Fall, Chandar & Whitmore 2005), leaving only small bound cores (e.g., Kroupa, Aarseth & Hurley 2001) or perhaps no bound cores at all. Some giant star forming regions, such as NGC 604 in M33, appear to have no clusters or cluster remnants, as if all star formation were isolated or initially unclustered. Maíz-Apellániz (2001) studied several other super-OB associations of this type. Such diversity in initial clustering follows from the hierarchical model if the average cloud density varies. Stars presumably form in similar cores everywhere, with pre-collapse densities of $10^5 - 10^8 \text{ cm}^{-3}$, but where the average density is low because of a low pressure ISM, for example, then the mass fraction of star-forming clumps can be low even in the densest regions of molecular clouds (which are not very dense in this case). Stars will still form clustered, and the efficiency will still be highest in the core regions, but this peak efficiency may be only $\sim 10\%$ rather than $\sim 50\%$. In that case there is not enough gravitational binding from stars alone to make a bound cluster when the gas leaves. Thus the hierarchical model predicts that the fraction of stars forming in initially bound clusters should depend on the local ISM pressure or density. This prediction is consistent with the observation by Larsen & Richtler (2000), who found that the fraction of uv light from stars in clusters increases with star formation rate, considering that star formation rate increases with gas column density and therefore ISM pressure.

1.6. Origins of Hierarchical Structure

The origin of hierarchical structure in interstellar gas is probably a combination of gravitational fragmentation and turbulence compression. Both produce scale-free density structures in regions where the total energy density is much larger than the thermal pressure. This inequality holds for most of the diffuse interstellar medium and much of the self-gravitating ISM because collisional cooling rates are high enough, and background heating rates are low enough, that the temperatures and thermal pressures are usually very low. Motions from various kinematic energy sources are then supersonic, and the mixture of these motions, particularly with the velocity-size correlation that results, produces correlated density structures. In the high density parts of these structures,

where self-gravity exceeds the background tidal force and the high column density provides some shielding from both radiative and kinematic energies, the gas has time and freedom to collapse into stars. The correlated density ensures that most of these collapses will be clustered together, in patches of various size, and it also provides the self-gravity that forces orbital mixing and self-binding to make a homogeneous embedded young cluster.

As mentioned in Section 1.2., not every cloud is surrounded by a larger cloud in a Russian doll pattern. Some small clouds are to the side of larger clouds and others may be between large clouds, with no obvious connection to one or the other. When clouds get pushed around by directed stellar pressures, the structures that form by gravity and turbulence get modified and cloud pieces can scatter anywhere. In this sense, it is not uncommon for stars to form in isolation or in small unbound groups that are far from clusters and associations. It appears for our Galaxy that the fraction of stars forming in this isolated fashion is small, perhaps 10% or less (Carpenter 2000). Recent Spitzer Space Telescope observations of the Perseus cloud suggest that $\sim 60\%$ of Class I protostars are outside the massive cores; many of these could still be in low-mass subclusters (Jorgensen et al. 2006).

1.7. Hierarchical Structure in the Galaxy NGC 628

Figure 1 shows a fractal Brownian motion model of a face-on galaxy compared to observations of the cluster size function in the galaxy NGC 628. On the left, a grayscale image of a model galaxy is shown, with four gray levels corresponding to different ratios of the density to the peak density (this figure is explained more completely and shown in color in Elmegreen et al. 2006). The darkest regions around the edges have the lowest projected densities, between 0.3 and 0.4 of the peak, the light gray regions inside of these have projected densities between 0.4 and 0.5 of the peak, whitish regions are between 0.5 and 0.6, and the dark gray regions inside the white regions have the highest densities, greater than 0.6 times the peak. The model is initialized in a 3D cube where the density probability distribution function is log-normal and the 3D power spectrum of density is approximately a power law with a slope of $-11/3$. This power spectrum is comparable to that for velocity and passive scalar density in Kolmogorov incompressible turbulence (it is also the best fit to the data compared to other power spectra that vary by ± 1 in slope). The cube is then multiplied by a Gaussian on the line of sight in order to simulate a projected galaxy disk.

The panel on the right of Figure 1 shows cumulative size distribution functions for connected regions, or “clouds” that were found objectively, for the same 4 levels of density threshold relative to the peak. The lowest curve (i.e., having the smallest count) is for the highest density threshold, greater than 0.6 times the peak. The crosses are B-band observations of the size distribution function for star-forming regions in an HST image of NGC 628 (with arbitrary shifts in each axis to fit the model). The physical scale ranges from 5 pc to 155 pc. The size distribution is a power law with a slope of -1.5 on this cumulative plot. The models match the observations. This cumulative size distribution corresponds to the differential function $n(R)dR \propto R^{-2.5}dR$.

The size distribution for loose stellar groupings in NGC 628 is approximately a power law from 2.5 pc to 150 pc (Elmegreen et al. 2006). This size range

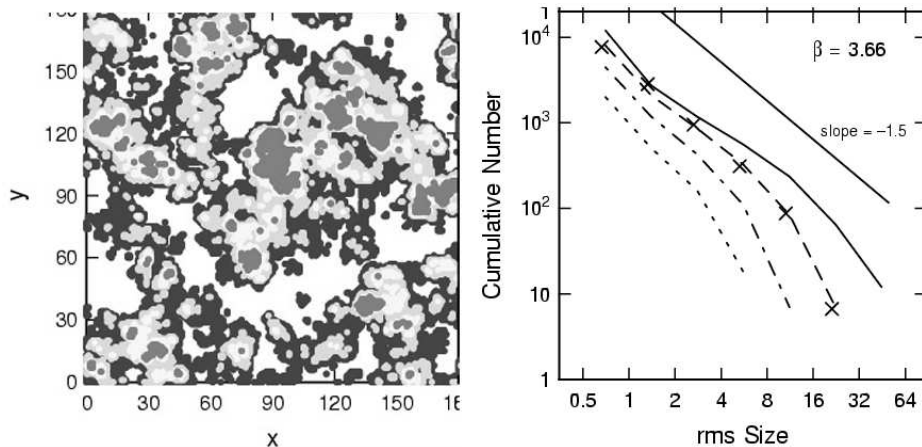


Figure 1. Fractal Brownian motion model (left) of a projected galaxy and cumulative size distribution functions (right) for clouds. The crosses are B-band data from HST images of the galaxy NGC 628, corresponding to objects with diameters ranging between 5 and 155 pc. The cumulative size distribution is a power law with a slope of -1.5 . The best model has a density power spectrum comparable to the power spectrum of Kolmogorov turbulence. (From Elmegreen et al. 2006.)

is larger than that for bound clusters, so it is interesting to ask whether the size distribution for loose groupings is a continuation of the size distribution for dense clusters. There is preliminary evidence for this from the cluster size distribution in Bastian et al. (2005), who studied M51. They derived a size function $n(R)dR \propto R^{-2.2}dR$, which is similar to that on larger scales. The analogy between unbound groupings and dense clusters is not straightforward, however, because the unbound groupings have a mass that increases with size approximately as $M \propto R^{1.5}$ (Elmegreen et al. 2006). This mass-size relation, along with the size distribution function, is consistent with a hierarchical star distribution with projected fractal dimension $D = 1.5$. That is, for a fractal, we expect $M \propto R^D$ and $n(R)dR \propto R^{-D-1}$ (Mandelbrot 1983). The problem with this is that the mass depends very little on radius in the dense clusters studied by Bastian et al. (2005). The lack of a correlation between mass and radius is also present in the data in Testi, Palla & Natta (1999) and Larsen (2004).

2. The Cluster Mass Function

There are only a few observations of the mass distribution functions of clusters. There are many observations of luminosity distribution functions, but mass distribution functions are more difficult to obtain because they require the additional knowledge of cluster ages. The complete mass function also requires the conversion between luminosity and mass as a function of age. Here we define the negative slope of the cluster mass function to be β , so $M^{-\beta}dM$ is proportional to the number of clusters with masses between M and $M + dM$. A histogram of the mass function plotted in equal intervals of $\log M$, which is the most common way to display the mass function, would then have a negative slope of $\beta - 1$.

The most complete cluster sample for a nearby galaxy is in the Large Magellanic Clouds. Elson & Fall (1985) measured the cluster luminosity function in the LMC and got $L^{-1.5}dL$ for a mixture of ages. Elmegreen & Efremov (1996) determined the luminosity functions of LMC clusters in four age intervals and found them all to be about $L^{-2}dL$. As the age was constant for each function, mass is proportional to luminosity. This means the mass distribution function is also a power law with the same slope, $M^{-2}dM$, giving $\beta = 2$. A similar study of LMC clusters by Hunter et al. (2003) found $\beta \sim 2$, while de Grijs & Anders (2006) obtained $\beta = 1.85 \pm 0.05$ using the same LMC data as in Hunter et al. but different age calibrations.

Cluster luminosity functions in the Milky Way have been determined for a long time, but not mass functions. One of the first modern determinations was by Battinelli et al. (1994), who derived a mass-luminosity relation for nearby Milky Way clusters and used this to get a mass function slope of $\beta = 2.13 \pm 0.15$ for the high mass end of the cluster mass function. Battinelli et al. also obtained $\beta = 2.04 \pm 0.11$ for clusters in Lynga's catalogue. For the Antenna galaxy, mass function slopes were found by Zhang & Fall (1999) to be $\beta = 1.95 \pm 0.03$ for young clusters and $\beta = 2.00 \pm 0.08$ for old clusters. For M51, cluster mass functions with $\beta = 2$ and various upper mass cutoffs were fitted to the observed luminosity functions in 3 HST passbands. Similarly in NGC 3310, $\beta = 2.04 \pm 0.23$ and in NGC 6745, $\beta = 1.96 \pm 0.15$ (de Grijs et al. 2003). These observations all imply that the cluster mass function is a power law with a slope β within several tenths of the value 2.0.

The same slope $\beta = 2$ is implied by galaxy-wide IMFs. Summed IMFs from clusters can produce a global IMF that is the same as the individual cluster IMF only if the cluster mass function slope is $\beta = 2$ or shallower. Observations suggest that galaxy-wide IMFs are indeed the Salpeter IMF, not much steeper, based on metallicity, color, H α equivalent width, and color-magnitude diagrams (Elmegreen 2006a). This is the case for the Milky Way bulge, dwarf galaxies, large galaxies, galaxy clusters, and the whole Universe. Because cluster IMF slopes average the Salpeter value too (Scalo 1998), the summed IMF equals the cluster IMF and the cluster mass function has to be close to M^{-2} . Even a slightly steeper value of $\beta = 2.3$ makes the summed IMF from clusters significantly steeper than the observed IMF of composite populations (Kroupa & Weidner 2003; Weidner & Kroupa 2005).

The cluster mass function is consistent with the theory of cluster formation discussed in the previous section. A hierarchical gas distribution, forming clusters at arbitrary levels in the hierarchy with a constant efficiency of star formation, has a mass function slope of exactly $\beta = 2$ (Fleck 1996). This can be seen from a simple tree model where there is one trunk with a mass of $N=16$, two branches off the trunk with masses of 8 each, two branches off each branch with masses of 4 each, two more branches off each of the previous with a mass of 2 each, and 16 total branches at the top of the tree with a mass of 1 each. The product of the number of branches times the mass of each branch is 16 for all levels in the hierarchy. There are $1 + 2 + 4 + 8 = 15 = N - 1$ possible branching points, each of which may be viewed as a possible cluster with all of the smaller branches inside of that cluster. If these 15 branching points are randomly sampled, then the probability that the chosen point is the trunk, giving a "cluster"

mass of 16, is 1/15. The probability the chosen mass is 8 is 2/15, the probability it is 4 is 4/15, and so on. Considering the log of the mass in base 2, the probability that the log is 4, so the mass is $2^4 = 16$, is 1/15. The probability the log is 3 is 2/15, etc.. In general, the probability that the log of the mass is A is $2^{4-A}/15$, or, more generally, $2^{N-A}/(2^N - 1)$. This probability is proportional to the count of branching points, and for the log mass expressions, the counting is for equal intervals of log mass ($dA = d\log_2 M$). Thus we have a probability function

$$P(M = 2^A) d\log_2 M = 2^{N-A}/(2^N - 1) d\log_2 M. \quad (1)$$

Converting A on the right-hand side back to mass, we get

$$P(M) d\log_2 M = \frac{2^N}{2^N - 1} M^{-1} d\log_2 M. \quad (2)$$

This equation shows that the mass distribution function of tree branches is proportional to M^{-1} for equal log intervals of mass, in which case $\beta - 1 = 1$ so $\beta = 2$. Sánchez, Alfaro, & Pérez (2006) show that the slope gets slightly shallower if blending effects are considered.

A similar result has been obtained for a smooth gas density distribution made by the fractal Brownian motion technique (Stützke et al. 1998; Elmegreen 2002a; Elmegreen et al. 2006). The mass function of three-dimensional clumps depends on the contour level used to define the clump and is steeper for denser levels. It is also steeper for steeper intrinsic power spectra (Stützke et al 1998). It varies from $\beta \sim 1.5$ for low density to $\beta \sim 2.3$ for high density when the fractal has a power spectrum with a power law slope equal to that of a passive scalar in incompressible Kolmogorov turbulence, and when the density has a log-normal probability distribution function. This variation in mass function slope with density is consistent with the observation that the mass function for giant molecular clouds is a shallow $\beta = 1.5$ to 1.8, and the mass function for clusters is steeper, $\beta = 1.8$ to 2.1. The difference is presumably because whole GMCs sample a lower density in the ISM than the star clusters they produce in their cores.

3. Massive Star Formation in Clusters and in the Field

An important question is whether massive stars can form in isolation, either in the remote field or on the peripheral regions of clusters. If massive stars need the cluster environment to accrete dense gas in a certain way, or to coalesce with other protostars, then there should not be many forming in low density regions (Testi, Palla, & Natta 1999). Of course, it is understood that all stars form in dense clumps, so the local environment is never low density, but the question is whether each massive star has a full complement of lower mass stars in the immediate neighborhood, filling out the IMF toward lower mass. An isolated dense clump could, in principle, form an isolated massive star without the thousands of other stars expected from the usual IMF.

The discussion in the previous section suggested that each logarithmic interval of cluster mass produces the same total stellar IMF, regardless of the cluster

mass itself. This is how the summed IMF can equal the individual cluster IMF: low mass clusters do not tip the balance toward exclusively low mass stars, for example (Elmegreen 2006a). The implication is that stars of any mass can form in clusters of any mass (provided the cluster mass exceeds the stellar mass). One condition for this to be true is that there is a universal IMF. If two or more star formation processes operate differently in different regions and if one tends to produce more high mass stars, then there are effectively two or more IMFs that have various contributions to the total depending on the environment (Elmegreen 2004). If the important environmental variable is density, for example, then low density clusters can have a slightly different IMF than high density clusters. With such dichotomy, it would no longer be true that stars of any mass form with equal probability in clusters of any mass (or density).

A test of these two possibilities is the “100-Taurus” test. For a universal IMF and $\beta \sim 2$, the summed IMF from 100 separate regions like the low mass Taurus clouds should have a slope that is only ~ 0.1 steeper than the IMF from one large region like Orion, which contains 100 times the mass of Taurus. Observations of IMFs in many low mass or low density regions like Taurus could settle this issue directly. If a given number of stars in Taurus-like regions have an IMF that is significantly steeper than the IMF from the same number of stars in Orion, or in the Orion Trapezium cluster, then there would seem to be at least two distinct IMFs, and massive stars would be favoring the higher mass and denser clusters.

At the moment, stars of any mass appear to form in clusters of any mass. One can then think of a cluster as “randomly” sampling a universal IMF. For purely random sampling, there is a very small chance that a massive star will form in a low-mass cluster, but most massive stars form in high mass clusters because most stars of all types form in high mass clusters. For the power-law part of the IMF, the maximum likely star mass out of N clusters of mass M equals the maximum likely star mass in one cluster of mass NM (Elmegreen 2006a). These statements are consistent with the observations by Oey, King & Parker (2004), who found the distribution of O-star counts per cluster in the LMC to be a power law with $\beta \sim 2$ down to a single O star. It is also consistent with a stronger statement by de Wit et al. (2005), who found that the total star mass in O-star containing clusters in the solar neighborhood is a power law with $\beta = 1.7$ down to a single O star (not just an O-star cluster containing other stars). This power law is similar to that for whole clusters, suggesting that sometimes a single O star can form in place of a cluster that has many smaller stars but the same total mass. The de Wit et al. observation is consistent with 4% of O-type stars forming in isolation or in peripheral regions of clusters.

There are actually many examples where O-type stars form along the periphery of massive dense clusters. Sequential triggering has this effect, and in the 30 Dor region of the LMC it is particularly clear (Walborn et al. 1999; see plot of massive stars in Elmegreen 2006b).

4. Cluster Disruption

There are several reasons why clusters eventually come apart. Gas dispersal in the first 1 to 3 My leads to decreased gravitational binding for the initial

stellar speed, and this causes some stars to escape directly, in a crossing time or less (Lada, Margulis, & Dearborn 1984). Many OB associations and loose stellar groups could have been collections of embedded clusters several million years earlier. Kroupa, Aarseth & Hurley (2001) studied cluster expansion after rapid gas loss with a star formation efficiency of 30%. They found that as the cluster expands to a new equilibrium radius, some stars are lost quickly and some remain in a bound core. They suggested that a cluster like the Trapezium cluster in Orion can turn into an open cluster like the Pleiades after an amount of time has passed that is comparable to the age of the Pleiades.

Mass is also lost from a cluster in the form of stellar winds and supernovae during stellar evolution. It takes much longer for a significant mass to be lost by stellar evolution than by cloud core disruption. After a few tens of millions of years, the decreasing cluster mass produces an overall expansion (Terlevich 1987). Eventually, the cluster density gets so low that self-gravitational forces become comparable to or less than the background tidal force. Then the cluster disperses. This is the third mechanism of cluster destruction. Tidal interactions with dense clouds, spiral arms, the bulge, and the galactic disk all give a lower limit to cluster density for survival. The outer parts of the cluster are shed into a tidal tail at the radius of this density threshold. As the cluster density decreases, the tidal radius decreases too, so the bound part of the cluster shrinks while the stars in the outer parts expand. Detailed models of cluster disruption including evolution and tidal effects are in Baumgardt & Makino (2003).

Other talks at this conference consider cluster destruction in greater detail. In particular, the destruction of clusters by giant molecular clouds has recently been shown to be important by Gieles et al. (2006). For molecular clouds, the important quantity is the volume filling factor of molecular material with a density comparable to or greater than the cluster density. When a cluster enters this volume, it becomes tidally unbound for a time. Movement near these dense regions can energize the stellar orbits, leading to eventual destruction. More distant encounters with molecular clouds are less important than those with impact parameters comparable to the cloud radius. Intermediate mass clusters may be disrupted by only a few GMC encounters, while low and high mass clusters require many encounters. The destruction time for a cluster of mass M through multiple encounters was found to be

$$t_{dis} = 2 \left(\frac{\Sigma_{cloud} \rho_{cloud}}{5.2 \text{ M}_{\odot}^2 \text{ pc}^{-5}} \right)^{-1} \left(\frac{M}{10^4 \text{ M}_{\odot}} \right)^{\gamma} \text{ Gyr} \quad (3)$$

where $\gamma = 1 - 3\lambda$ and λ is the power in the cluster mass-radius relation, $R_{cluster} \propto M^{\lambda}$. The typical mass column density of a molecular cloud is Σ_{cloud} and the ISM-averaged density of GMCs is ρ_{cloud} . Gieles et al. (2006) suggest $\lambda \sim 0.13$ and $\gamma \sim 0.61$. Thus $t_{dis} \propto M^{0.61}$.

A similar mass dependence for the destruction time of a cluster has been found in other studies. Boutloukos & Lamers (2003) found the mass-dependent disruption time in four galaxies to be $t_{dis} \sim M^{0.6}$. Gieles et al. (2004) showed that models by Baumgardt & Makino (2003) were consistent with $t_{dis} \sim M^{0.64}$. De la Fuente Marcos & de la Fuente Marcos (2004) used dynamical models to suggest $t_{dis} \sim M^{0.68}$. Most recently, Lamers et al. (2005) compared $M(t)$ from numerical experiments using this power law form for $t_{dis} = M^{\gamma}$ and the simple

model $dM/dt = -M/t_{dis}$. The model and analytical results were in excellent agreement for $\gamma = 0.62$.

If t_{dis} depends on cluster mass, then the mass function of clusters should get shallower at low mass over time because the lowest mass clusters get destroyed soonest. After a while, the slope of the cluster mass function should approach $\beta = 1 - \gamma = 0.38$ at low mass (Lamers et al. 2005). Recall that β is defined to be the negative value of the slope on a plot of the cluster mass spectrum in linear mass intervals, and $\beta - 1$ is the slope on a spectrum in log mass intervals. A value of $\beta = 0.38$ implies that a histogram of cluster number in equal intervals of log mass should increase with log M at low M , reach a peak, and then decrease with log M as $M^{-(\beta-1)}$ for sufficiently large mass where destruction has not been significant yet. Most cluster mass functions plotted with log M intervals are indeed peaked like this, with a rising part at low log M , but this is always attributed to magnitude limits in the observations. That is, the turnover toward low mass is the result of missing clusters that are present but too faint to discern. For example, de Grijs & Anders (2006) plotted histograms of cluster counts in log M intervals for the LMC and found continuous power law functions down to and below $10^4 M_{\odot}$ for ages up to $10^{9.75}$ years (this was also the case in Elmegreen & Efremov [1996] and Hunter, et al. [2003]). There is no evidence for a mass-dependent destruction in these data.

In contrast, Fall, Chandar & Whitmore (2005) suggest that the destruction rate is independent of cluster mass, and that the mass function stays constant over time, which is consistent with the observation by de Grijs & Anders (2006) and also with observations of the Antennae galaxy by Fall et al. Fall et al. find that the number of clusters in intervals of equal age decreases inversely with the age, independent of cluster mass. This decrease is somewhat continuous over time all the way from 10^6 years to 10^9 years. This is a surprising result because there is not even a feature in this trend where the mechanism of cluster disruption is expected to change from gas expulsion to stellar evolution.

In the Fall et al. model, we can write the number of clusters more massive than M_0 as $n_{M>M_0}(t) \propto t^{-1}$. If the observations also suggest that the form of the mass function does not change over time and is $n(M) = n_0 M^{-2}$ for linear intervals of M , then

$$\int_{M_0}^{\infty} n_0 M^{-2} dM = n_0 M_0^{-1} \propto t^{-1} \quad (4)$$

for constant lower detection limit M_0 . Thus $n_0 \propto t^{-1}$, the maximum cluster mass is $\propto t^{-1}$, and each cluster has its mass decrease as t^{-1} . We also obtain that $t_{dis} \propto M^{-1}$ from the relations $dM/dt \equiv -M/t_{dis} \propto t^{-2} \propto M^2$, or $d \log M / d \log t = -1$.

Why is there a difference between the Fall et al. (2006) model and the Lamers et al. (2005) model? The key observation to distinguish between these two models is the slope of the cluster mass function versus time.

5. Conclusions

The ISM and star birth positions appear scale-free from the scale of the Jeans length in the ambient ISM (on a kpc scale) to below the star formation scale. This scale-free distribution is not likely to be continuous in any one region,

but still present on average, and present in a piecewise sense. Stars form in dense clumps whose local mass fraction compared to the surrounding molecular material is high and whose mixing time is relatively short. The mixed young stars are the “cluster.” Gas removal stops star formation in the dense core but not everywhere. It often continues on the periphery of the cluster and in the remaining molecular cloud as a result of sequential triggering. This basic model explains the cluster mass spectrum, the galactic star formation rate and star formation timescale (not discussed here; see Elmegreen 2002b), and the observed stellar grouping structures. It does not give the independence between cluster mass and size, however, which presumably involves additional physical processes.

Cluster mass loss is dominated by gas disruption and stellar evolution at first, by tidal shredding from giant molecular clouds and spiral density waves after a while, and by thermal disruption on the longest time scale. The disruption time varies with cluster mass, but the exact scaling relationship is subject to debate. Observations suggest that the power-law form of the cluster mass distribution function is preserved for at least 10^9 years in some galaxy disks, in which case the disruption time is either longer than this or it does not scale positively with mass in a noticeable way.

References

- Bastian, N., Gieles, M., Efremov, Yu. N., Lamers, H. J. G. L. M. 2005, *A&A*, 443, 79
 Battinelli, P., Brandimarti, A., & Capuzzo-Dolcetta, R. 1994, *A&AS*, 104, 379
 Baumgardt, H., & Makino, J. 2003, *MNRAS*, 340, 227
 Blitz, L., & Rosolowsky, E. 2006, *ApJ*, in press
 Bonnell, I. A., Bate, M. R., & Vine, S. G. 2003, *MNRAS*, 343, 413
 Boulanger, F., & Viallefond, F. 1992, *A&A*, 266, 37
 Boutloukos, S. G., & Lamers, H. J. G. L. M. 2003, *MNRAS*, 338, 717
 Carpenter, J.M. 2000, *AJ*, 120, 3139
 Dahm, S.E., & Simon, T. 2005, *AJ*, 129, 829
 de Grijs, R., Anders, P., Bastian, N., et al. 2003, *MNRAS*, 343, 1285
 de Grijs, R. & Anders, P. 2006, *MNRAS*, 366, 295
 de La Fuente Marcos, R., & de La Fuente Marcos, C. 2004, *New Astron.*, 10, 53
 de Wit, W. J., Testi, L., Palla, F. & Zinnecker, H. 2005, *A&A*, 437, 247
 Dickey, J.M., McClure-Griffiths, N.M., Stanimirovic, S., Gaensler, B.M, & Green, A.J, 2001, *ApJ*, 561, 264
 Efremov, Y.N. 1995, *AJ*, 110, 2757
 Efremov, Y.N., & Elmegreen, B.G. 1998, *MNRAS*, 299, 588
 Elmegreen, B.G. 1993, *ApJ*, 411, 170
 Elmegreen, B.G. 2000, *ApJ*, 530, 277
 Elmegreen, B.G. 2002a, *ApJ*, 564, 773
 Elmegreen, B.G. 2002b, *ApJ*, 577, 206
 Elmegreen, B.G. 2004, *MNRAS*, 354, 367
 Elmegreen, B.G. 2006a, *ApJ*, 648, in press
 Elmegreen, B.G. 2006b, in *Massive Stars: From Pop III and GRBs to the Milky Way*, ed. Livio, M., et al., Cambridge: Cambridge Univ. Press, in press
 Elmegreen, B.G., & Elmegreen, D.M. 1987, *ApJ*, 320, 182
 Elmegreen, B.G., Leitner, S.N., Elmegreen, D.M., & Cuillandre, J.-C. 2003, *ApJ*, 593, 333
 Elmegreen, B.G., Elmegreen, D.M., Chandar, R., Whitmore, B., & Regan, M. 2006, *ApJ*, 644, 879

- Elmegreen, B.G., & Efremov, Y.N. 1996, *ApJ*, 466, 802
Elmegreen, B.G., & Efremov, Y.N. 1998, *ApJ*, 480, 235
Elson, R. A. W., & Fall, S. M. 1985, *ApJ*, 299, 211
Fall, S.M., Chandar, R., & Whitmore, B.C., 2005, *ApJL*, 631, 133
Fleck, R.C., Jr. 1996, *ApJ*, 458, 739
Gieles, M., Baumgardt, H., Bastian, N., Lamers, H. J. G. L. M. 2004, in *The Formation and Evolution of Massive Young Star Clusters*, ASP Conference Series, Vol. 322. Ed. H.J.G.L.M. Lamers, L.J. Smith, & A. Nota, San Francisco: Astronomical Society of the Pacific, p. 481
Gieles, M., Portegies Zwart, S. F., Baumgardt, H., Athanassoula, E., Lamers, H. J. G. L. M., Sipior, M., & Leenaarts, J. 2006, *MNRAS*, in press.
Grabelsky, D. A., Cohen, R. S., Bronfman, L., Thaddeus, P., & May, J. 1987, *ApJ*, 315, 122
Hunter D. A., Elmegreen B. G., Dupuy T. J., & Mortonson M., 2003, *AJ*, 126, 1836
Ivanov, G.R. 2005, *Pub.Astr.Soc. Rudjer Boskovic*, 5, 75
Jorgensen, J.K., et al. 2006, *ApJ*, 645, 1246
Kroupa, P., Aarseth, S., & Hurley, J 2001, 321, 699
Kroupa, P., & Weidner, C. 2003, *ApJ*, 598, 1076
Lada, C. J., Margulis, M. & Dearborn, D., 1984, *ApJ*, 321, 141
Lada, C.J., & Lada, E.A. 2003, *ARAA*, 41, 57
Lamers, H. J. G. L. M., Gieles, M., Bastian, N., Baumgardt, H., Kharchenko, N. V., & Portegies Zwart, S. 2005, *A&A*, 441, 117
Larsen, S. S., & Richtler, T. 2000, *A&A*, 354, 836
Larsen, S.S. 2004, *A&A*, 416, 537
Maíz-Apellániz, J. 2001, *ApJ*, 563, 151
Mandelbrot, B.B. 1983, *The Fractal Geometry of Nature*, San Francisco: Freeman.
Matzner, C.D., & McKee, C.F. 2000, *ApJ*, 545, 364
McGee, R.X. & Milton, J.A. 1964, *Austr. J. Physics*, 17, 128
Myers, P. C., Evans, N. J., II, & Ohashi, N. 2000, in *Protostars and Planets IV*, ed. V. Mannings, et al., Tucson: Univ. of Arizona, 217
Oey, M. S., King, N. L. & Parker, J. Wm. 2004, *AJ*, 127, 1632
Sánchez, N., Alfaro, E.J., & Pérez, E. 2006, *ApJ*, 641, 347
Scalo, J.M. 1998, in *The Stellar Initial Mass Function*, ed. G. Gilmore, I. Parry & S. Ryan, Cambridge: Cambridge University Press, p. 201
Smith, M.D., Gredel, R., Khanzadyan, T. et al. 2005, *MmSAI*, 76, 247
Stützkki, J., Bensch, F., Heithausen, A., Ossenkopf, V., & Zielinsky, M. 1998, *A&A*, 336, 697
Terlevich, E. 1987, *MNRAS*, 224, 193
Testi, L., Sargent, A.I., Olmi, L., & Onello, J.S. 2000, *ApJL*, 540, 53
Testi, L., Palla, F. & Natta, A. 1999, *A&A*, 342, 515
Walborn, N.R., Barbá, R.H., Brandner, W., Rubio, M., Grebel, E.K. & Probst, R.G. 1999, *AJ*, 117, 225
Walsh, A.J., Bourke, T.L., & Myers, P.C. 2006, *ApJ*, 637, 860
Weidner, C., & Kroupa, P. 2005, *ApJ*, 625, 754
Zhang, Q., & Fall, S.M. 1999, *ApJL*, 527, 81